



# Charge transport and near-infrared emission properties of semiconducting polymers

Tsuyoshi Michinobu <sup>1</sup>

Received: 21 April 2023 / Revised: 27 May 2023 / Accepted: 1 June 2023 / Published online: 26 June 2023

© The Author(s) 2023. This article is published with open access

## Abstract

Research on semiconducting polymers is an interdisciplinary field that requires a wide range of knowledge ranging from polymer syntheses to electronics applications. Clarifying the correlations between chemical structures and physical properties leads to a better understanding of these materials. To find suitable application fields, it is necessary to repeatedly prepare polymer samples with slightly different chemical structures and evaluate their physical properties. The author's group started their research with the aim of developing high-performance semiconducting polymers that exhibited high charge carrier mobilities in thin film transistors, and this has recently been expanded to polymers that emit light in the near-infrared region.

## Introduction

Similar to silicon, organic semiconductors with *p*-type semiconducting properties transport holes, and those with *n*-type semiconducting properties transport electrons. They can be used in organic electronic devices, including solar cells and thin-film transistors, and have garnered significant interest in both fundamental science and applied research. This is partly because organic semiconductors can be implemented into flexible and stretchable electronics. Fine control of the weak intermolecular interactions in supramolecular chemistry enables the production of self-healing organic electronic devices, which is difficult to achieve with silicon-based devices. It is apparent from many studies of organic semiconductors that the development of *n*-type semiconducting polymers has lagged behind that of *p*-type semiconducting polymers [1]. While hole mobilities exceeding  $10 \text{ cm}^2 \text{ V}^{-1} \text{ s}^{-1}$  have been reported for some

*p*-type semiconducting polymers [2], such high mobilities are not easily obtained for *n*-type semiconducting polymers. This is due to the difficult molecular design and the fact that *n*-type semiconductors are intrinsically unstable under atmospheric conditions.

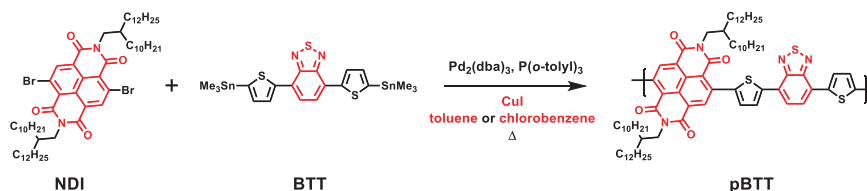
There are several methods used for evaluating charge transport, but in this study, bottom-gate top-contact thin-film transistors were fabricated and evaluated. A series of studies has shown that the mobilities mainly depended on the polymer crystallinity and that the direction of charge transport depended on the polymer orientation. Since it is not possible to make a single polymer that is long enough to connect electrodes several millimeters in length, the charge carriers proceed by hopping in the  $\pi$ - $\pi$  stacking direction of the polymer. Accordingly, the higher the crystallinity and the shorter the  $\pi$ - $\pi$  stacking distance, the higher the mobility. In the case of transistors, edge-on orientations are more suitable than face-on orientations because the carriers flow between the electrodes in a direction horizontal to the gate electrode [3]. In the following sections, thin film transistors of organic semiconducting polymers that were developed in my laboratory are shown. After optimization of the polymer structures, some of the highest electron mobilities known for thin film transistors were achieved (Supporting Information). Finally, the near-infrared emission properties of some narrow band gap polymers, which were found during the course of this study, are introduced.

**Supplementary information** The online version contains supplementary material available at <https://doi.org/10.1038/s41428-023-00807-3>.

✉ Tsuyoshi Michinobu  
michinobu.t.aa@m.titech.ac.jp

<sup>1</sup> Department of Materials Science and Engineering, Tokyo Institute of Technology, 2-12-1 Ookayama, Meguro-ku, Tokyo 152-8552, Japan

**Scheme 1** Polymerization of NDI and BTT monomers to form **pBTT**



## Effect of molecular weight on the transistor performance

First, naphthalenediimide (NDI) and benzothiadiazole (BT) were chosen as common acceptors with which to produce crystalline polymers, and the resulting donor-acceptor type polymers **pBTT** were designed and synthesized via Pd-catalyzed Stille polycondensation (Scheme 1) [4]. The polymerization conditions were initially optimized. When the solvent was changed from toluene to chlorobenzene, the number-average molecular weight ( $M_n$ ) of the resulting polymer increased from 29.8 to 67.5 kg mol<sup>-1</sup> due to the higher solubility in chlorobenzene (entry 2, Table 1). It was also found that a small amount of CuI improved the catalytic efficiency and furnished a higher molecular weight polymer with a  $M_n$  of 74.8 kg mol<sup>-1</sup> (entry 3, Table 1). The optimum CuI amount was determined to be 15 mol%, and it yielded a polymer with a  $M_n$  of 116.4 kg mol<sup>-1</sup> (entry 5, Table 1).

As there was a series of **pBTTs** with different molecular weights, the effect of the molecular weight on charge transport in the thin film transistors was investigated. A bottom-gate top-contact device was fabricated by spin-coating a **pBTT** solution on an octadecyltrimethoxysilane (OTMS)-treated n<sup>+</sup>-Si/SiO<sub>2</sub> substrate followed by thermal annealing under optimized conditions. This polymer exhibited ambipolar properties, i.e., it transported both holes and electrons. The carrier mobilities were plotted as a function of the molecular weight (Fig. 1). Both the hole and electron mobilities increased with increasing molecular weight and reached maxima at a molecular weight of just under 90,000. The polymer synthesized in chlorobenzene with 10 mol% CuI exhibited an optimized hole mobility ( $\mu_h$ ) of 0.92 cm<sup>2</sup> V<sup>-1</sup> s<sup>-1</sup> and an electron mobility ( $\mu_e$ ) of 0.19 cm<sup>2</sup> V<sup>-1</sup> s<sup>-1</sup>. Recently, there was a similar report indicating that the critical polymerization degree leading to maximum charge carrier mobilities was in the range of 45–60 repeat units [5]. This can be explained by the fact that in the low molecular weight range, the crystalline domains did not grow sufficiently, which resulted in low mobility, while in the high molecular weight range, the polymer chains were too highly entangled, which suppressed intermolecular charge transport via  $\pi$ - $\pi$  interactions.

**Table 1** Polymerization conditions for the NDI and BTT monomers<sup>a</sup>

Entry	Solvent	CuI (mol%)	$M_n$ (kg mol <sup>-1</sup> ) <sup>b</sup>	$M_w/M_n^c$	Yield (%) <sup>d</sup>
1	Toluene	0	29.8	2.6	48
2	Chlorobenzene	0	67.5	3.3	58
3	Chlorobenzene	5	74.8	3.0	78
4	Chlorobenzene	10	86.0	3.1	84
5	Chlorobenzene	15	116.4	3.4	92
6	Chlorobenzene	20	92.5	3.2	86

<sup>a</sup>Polymerization was performed under reflux in the presence of Pd<sub>2</sub>(dba)<sub>3</sub> (3 mol%) and P(*o*-tolyl)<sub>3</sub> (12 mol%) for 48 h under N<sub>2</sub>

<sup>b</sup>Number-average molecular weight

<sup>c</sup>Polydispersity index

<sup>d</sup>Yield of **pBTT**

## From benzothiadiazole to benzobisthiadiazole

Next, BT was replaced with a stronger acceptor, namely, benzobisthiadiazole (BBT). BBT was first reported by Yamashita in 1994 [6], but its semiconducting polymers were not realized for more than a decade. In 2011, Wudl et al. reported the first BBT-based semiconducting polymers [7–9]. A series of BBT-based semiconducting polymers displayed ambipolar-type transistor properties with mobilities exceeding 1.0 cm<sup>2</sup> V<sup>-1</sup> s<sup>-1</sup>. However, there was room for improvement in the thin film crystallinity and the on/off ratios of their transistors. The first BBT-based polymer developed by our group was **PBBT-Tz-FT**, which had the highest occupied molecular orbital (HOMO) level of -5.42 eV and the lowest unoccupied molecular orbital (LUMO) level of -3.80 eV (Fig. 2) [10]. Because these HOMO and LUMO levels were suitable for charge injection, the thin film transistor based on this polymer exhibited ambipolar behavior. The as-cast film showed a hole mobility ( $\mu_h$ ) of 1.7 × 10<sup>-3</sup> cm<sup>2</sup> V<sup>-1</sup> s<sup>-1</sup> and an electron mobility ( $\mu_e$ ) of 1.3 × 10<sup>-3</sup> cm<sup>2</sup> V<sup>-1</sup> s<sup>-1</sup>. Thermal annealing improved the crystallinity of the polymer thin film, resulting in an increase in the mobility. The optimum annealing temperature was approximately the glass transition temperature of 170 °C, and  $\mu_h$  and  $\mu_e$  were 6.8 × 10<sup>-3</sup> cm<sup>2</sup> V<sup>-1</sup> s<sup>-1</sup> and 1.5 × 10<sup>-2</sup> cm<sup>2</sup> V<sup>-1</sup> s<sup>-1</sup>, respectively.

One of the sulfur atoms in BBT was then substituted with another atom. For example, **PSeS** was synthesized by

replacing a S with Se, which produced a localized LUMO on the triply fused conjugated framework. Accordingly, this change resulted in a deeper LUMO level of  $-3.86$  eV. Deeper LUMOs generally increase the electron injection efficiency and improve the electron mobility. The thin film transistor based on **PSeS** displayed an improved  $\mu_e$  of  $0.087$   $\text{cm}^2 \text{V}^{-1} \text{s}^{-1}$  [11].

Similar to the Se substitution, one of the S atoms in BBT was replaced by nitrogen to produce thiadiazolobenzotriazole and the corresponding polymer, **PSN**. It was found that the  $\text{sp}^3$  hybridized nitrogen atoms increased the electron-donating properties due to an inductive effect, which elevated the HOMO level. **PSN** had a shallow HOMO level of  $-5.21$  eV, which facilitated hole injection and improved the  $\mu_h$  by approximately 100 times to  $0.65$   $\text{cm}^2 \text{V}^{-1} \text{s}^{-1}$  [11].

Nitrogen substitution exhibited another good characteristic: it could introduce an additional alkyl side chain on the nitrogen atom. Since the BBT unit has low solubilities in common organic solvents, alkylated thiophene rings are usually added to provide sufficient solubility. However, it has been noted that this alkyl chain creates steric hindrance with the comonomer unit and reduces the backbone

planarity of the polymer main chain. To solve this problem, the octyl chains introduced into the thiophene rings were removed because the *N*-alkylated thiadiazolobenzotriazole unit provided sufficient solubility of the polymer in common organic solvents and enabled thin film fabrication by wet processes (Fig. 3a, b) [12]. This subtle change in the chemical structure caused significant improvements in the charge carrier mobilities of the transistors. It was found that the electron mobility was improved more than 1000-fold from  $10^{-3}$   $\text{cm}^2 \text{V}^{-1} \text{s}^{-1}$  for **pSN-NDI** to  $4.87$   $\text{cm}^2 \text{V}^{-1} \text{s}^{-1}$  for **pSNT** (Fig. 3a–c) [4]. Grazing-incidence wide-angle X-ray scattering (GIWAXS) measurements showed that the crystallinity of the polymer thin film was significantly changed. **pSN-NDI** was almost amorphous, whereas **pSNT** showed higher-order lamellar peaks and high crystallinity (Fig. 3d, e). The crystalline domains had a mixture of edge-on and face-on orientations and were capable of three-dimensional charge transport. The transistor performance suggested some hole transport in addition to electron transport.

To construct a unipolar *n*-channel transistor that completely blocked hole transport, the device structure was improved. A self-assembled monolayer, such as OTMS, is usually fabricated on top of the insulating  $\text{SiO}_2$  layer to control the wettability between the gate electrode and the semiconductor polymer. However, this monolayer cannot trap holes. In this case, an alkylamine, i.e., [3-(*N,N*-dimethylamino)propyl]trimethoxysilane (NTMS), was introduced on the surface of the self-assembled monolayer [4]. The few existing holes were then efficiently trapped by the amine moieties, resulting in only *n*-channel characteristics. As a result, the electron mobility was further improved to  $5.35$   $\text{cm}^2 \text{V}^{-1} \text{s}^{-1}$  (Fig. 3f).

Intramolecular hydrogen bonding was adopted to improve the planarity of the main chain backbone even further. By inserting a vinylene spacer into the polymer based on NDI and thiadiazolobenzotriazole (**pSNT**), intramolecular hydrogen bonds were formed in the main chain backbone of **P4** (Fig. 4) [13]. This resulted in a very high crystallinity for the thin film state. The distance for the  $\pi$ - $\pi$

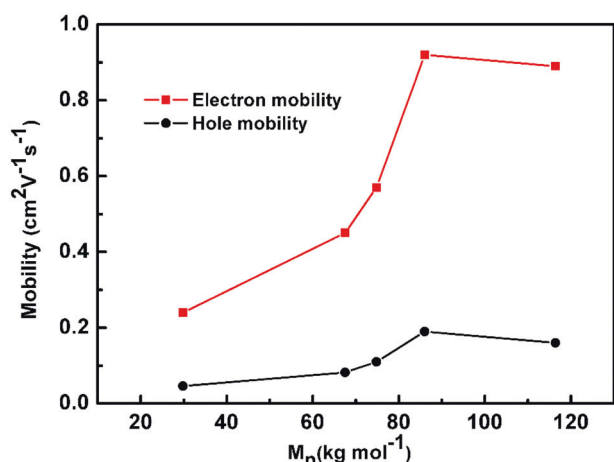


**Fig. 1** Relationship between the molecular weights ( $M_n$ ) and the charge carrier mobilities of thin film transistors based on **pBTT**

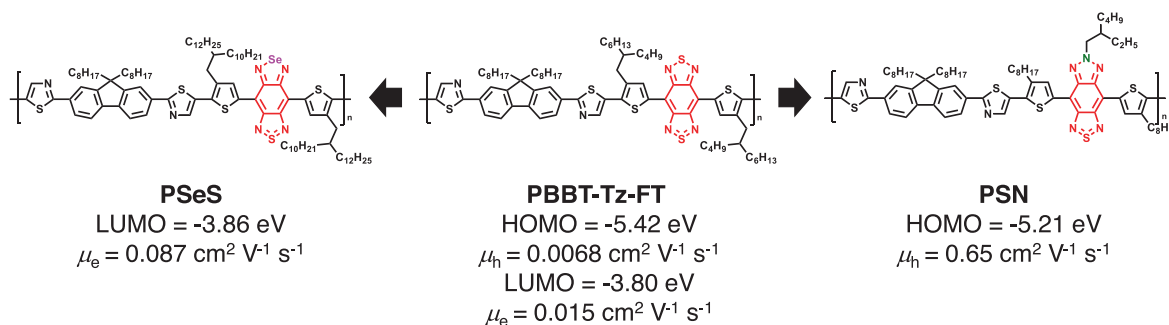
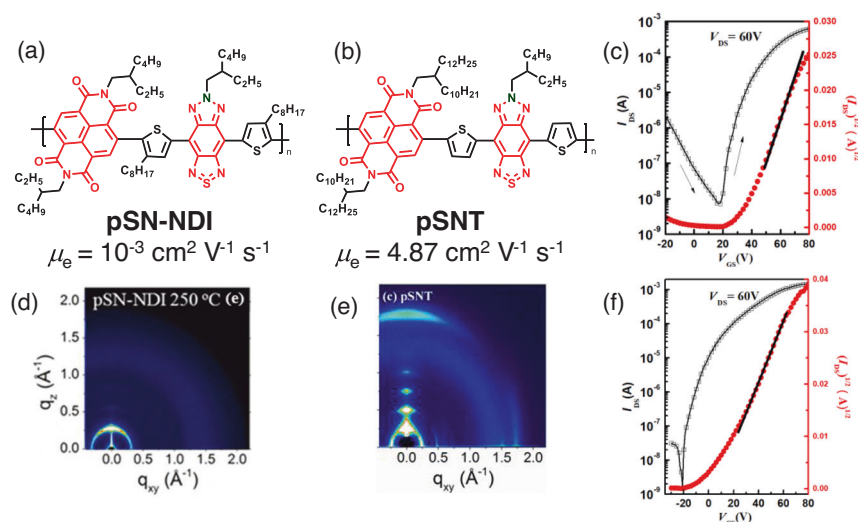


**Fig. 2** Effects of heteroatom substitution on the electronic states and thin film transistor mobilities

**Fig. 3** Chemical structures and electron mobilities of (a) **pSN-NDI** and (b) **pSNT**. c Transfer curve for **pSNT** fabricated on OTMS-treated  $\text{SiO}_2/\text{n}^{++}\text{-Si}$  under optimized conditions [12]. GIWAXS patterns for the thin films of (d) **pSN-NDI** [12] and (e) **pSNT** [4]. f Transfer curve for **pSNT** fabricated on NTMS-treated  $\text{SiO}_2/\text{n}^{++}\text{-Si}$  under optimized conditions [4].



interactions, which were estimated from the GIWAXS patterns, provided a good guide to estimate the thin film crystallinity and potentials of the charge carrier mobilities. Most crystalline semiconducting polymers display  $\pi$ - $\pi$  interaction distances of 3.6–3.7 Å, but this polymer exhibited a much shorter value of 3.40 Å. This result was consistent with the observed electron mobility. A thin film transistor based on this polymer showed unipolar *n*-channel charge transport properties with a  $\mu_e$  of  $7.16 \text{ cm}^2 \text{ V}^{-1} \text{ s}^{-1}$ . This value is one of the highest values reported for organic polymers.

Although optimization of the main backbones of polymers has already been discussed, the design of the side chain alkyl groups is also very important. Accordingly, the effects of substitution positions for the alkyl side chains on the transistor performance were investigated. The three polymers **P1**–**P3** shown in Fig. 5 had the same main chain backbone structures, but they differed in the number of alkyl side chains and their substitution positions [14]. For example, **P1** was highly soluble in common organic solvents (even in hexane) due to the presence of two types of alkyl side chains (the green and blue substituents in Fig. 5). In addition, this polymer exhibited a large torsional angle ( $\theta$ ) of  $53.0^\circ$  between the thienothiophene and thiophene moieties due to steric repulsion between these alkyl chains, which resulted in low crystallinity and a low hole mobility ( $\mu_h$ ) of  $1.94 \times 10^{-4} \text{ cm}^2 \text{ V}^{-1} \text{ s}^{-1}$  in the thin film transistor. To improve the thin film crystallinity, one of the alkyl chains (blue substituents in Fig. 5) was removed, which reduced  $\theta$  to  $31.0^\circ$  and increased  $\mu_h$  by a factor of 10 or more. Furthermore, when the position of the alkyl chain was changed (pink substituents in Fig. 5), the main chain backbone became nearly flat with a  $\theta$  of  $11.5^\circ$ , and  $\mu_h$  exceeded  $0.1 \text{ cm}^2 \text{ V}^{-1} \text{ s}^{-1}$ . All of these results suggested that the positions of the alkyl side chains had a significant impact on the planarity of the main chain backbone as well as the charge carrier mobilities.

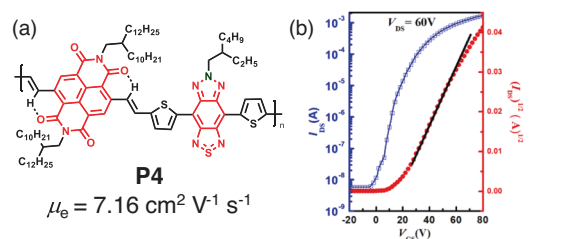


**Fig. 4** a Chemical structure and electron mobility and b transfer curve of **P4** under optimized conditions [13]. Copyright 2019 American Chemical Society

Next, the orientations of the polymer main chain backbone structures were successfully controlled by the lengths of the alkyl side chains. Although an edge-on orientation is desirable for the construction of high-performance organic transistors, there was no way to create it intentionally until recently [15]. Two polymers, **PSNVT-DTC16** and **PSNVT-DTC8**, were designed and synthesized (Fig. 6) [16]. It should be noted that they have the same main chain backbone structures, but the lengths of the alkyl side chains are different. For example, **PSNVT-DTC16** has two alkyl chains with approximately the same lengths, i.e., the  $\text{C}_{16}$  and  $\text{C}_{14}$  chains (green and blue substituents, respectively) (Fig. 6a). In this case, the GIWAXS pattern revealed that the polymer tended to adopt a face-on orientation suitable for organic photovoltaic applications. On the other hand, **PSNVT-DTC8** has different lengths for the alkyl chains, such as the  $\text{C}_8$  and  $\text{C}_{14}$  chains (green and blue substituents, respectively) (Fig. 6b). This polymer was more likely to adopt an edge-on orientation based on the GIWAXS pattern. This difference in the molecular orientation was also reflected in the transistor characteristics; **PSNVT-DTC16** had a moderate  $\mu_h$  of  $0.13 \text{ cm}^2 \text{ V}^{-1} \text{ s}^{-1}$ , while **PSNVT-DTC8** achieved a much higher  $\mu_h$  of  $3.22 \text{ cm}^2 \text{ V}^{-1} \text{ s}^{-1}$ .

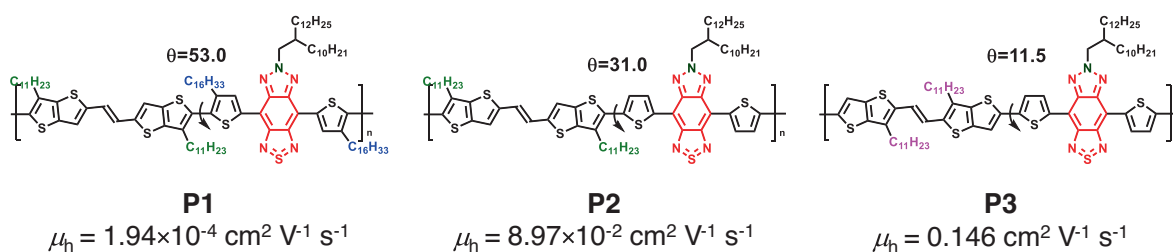
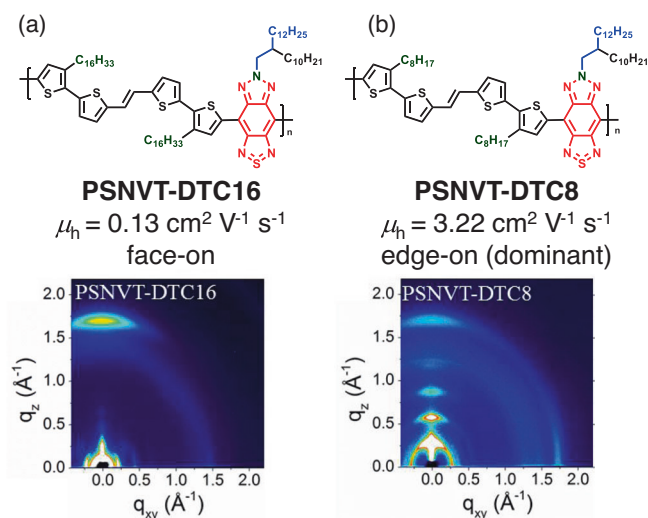


**Fig. 5** Effects of the positions of alkyl side chains on the backbone planarity and transistor mobilities. The torsional angles ( $\theta$ ) were estimated from DFT calculations of model oligomers

**Fig. 6** Chemical structures, transistor mobilities, and GIWAXS patterns for (a) PSNVT-DTC16 and (b) PSNVT-DTC8 [16]. Copyright 2017 Wiley



In addition, high stability must be achieved under atmospheric conditions for practical applications. One of the degradation mechanisms for *n*-channel organic transistors involves a reaction with water. To avoid this, it is said that the LUMO levels of organic semiconductors must be lower than  $-4.0 \text{ eV}$  [17]. In this context, all-acceptor copolymers with very deep LUMO levels were designed and successfully synthesized by using an environmentally friendly polymerization method called direct arylation polymerization (Fig. 7a). A thiophene unit with a reactive C-H bond is commonly employed in direct arylation polymerizations, but this study demonstrated that an electron-accepting unit of the thiazole was also employed to produce the electron-deficient copolymer **P2** with a LUMO level of  $-4.0 \text{ eV}$  [18]. It was recently demonstrated that the same strategy can be applied to other electron-deficient aromatic ring monomers, such as oxazoles, to yield the corresponding copolymers [19]. As the thin film of **P2** showed good crystallinity, the transistor displayed an electron mobility of  $1.87 \text{ cm}^2 \text{ V}^{-1} \text{ s}^{-1}$ . It is noteworthy that even after a month of exposure to air at room temperature, it maintained a mobility of more than  $1.0 \text{ cm}^2 \text{ V}^{-1} \text{ s}^{-1}$  (Fig. 7b). In addition, no degradation was observed even after approximately 100 cycles of voltage application, indicating the extremely

high stability of this polymer device (Fig. 7c). The versatility of the all-acceptor molecular design for high-performance *n*-type semiconductors was also recently proven by using small molecules. An *n*-channel transistor based on the NDI-thiadiazolobenzotriazole-NDI semiconductor exhibited high air stability [20].

## Conjugated polymer nanoparticles

Semiconductor polymers, also called conjugated polymers, are known for their luminescent properties. They have been used as the emitting layers of organic light emitting diodes, chemosensors, and biosensors [21–23]. It is well known that the crystalline regions of conjugated polymers provide quenching site when they aggregate. However, it was found that relatively high fluorescence quantum yields were maintained even in the solid-state by adopting conjugated polymers with nonplanar backbone structures. In this study, the molecular design and functionalization of an electron-rich carbazole unit was noted. For example, 2,7-carbazole-based donor-acceptor copolymers are often employed to form crystalline and high-mobility polymers due to the linear structure of the 2,7-carbazole connectivity.



On the other hand, it was demonstrated that 1,8-carbazole-based copolymers were highly distorted due to the 1,8-carbazole structure [24–26]. The 1,8-carbazole-based copolymers thus showed lower crystallinities and relatively higher fluorescence quantum yields in the aggregated state. These polymers were converted into nanoparticles by reprecipitation and employed in bioimaging applications [27]. The selection of appropriate acceptor units enabled emission in the near-infrared region, which is classified as the window for living organisms. A correlation between the fluorescence peak positions and the quantum yields was investigated comprehensively (Fig. 8) [28]. For example, use of the BBT acceptor produced emission at wavelengths >1000 nm. In addition, the 1,8-carbazole-based nonplanar conjugated polymers exhibited noticeable advantages for various applications. Highly crystalline conjugated polymers, such as **PSN** and **PSeN**, showed drastic decreases in the fluorescence quantum yields when polymer nanoparticles were formed (see red circles in Fig. 8). However, the 1,8-carbazole-based BBT polymer displayed a slight decrease in the fluorescence quantum yield in almost the same wavelength range (blue circles in Fig. 8). Since these organic polymer-based

nanoparticles do not contain toxic elements such as quantum dots, they are expected to enable safe bioimaging.

## Conclusions

It was shown that the semiconducting properties of conjugated polymers can be controlled by molecular design. To achieve excellent transistor performance with semiconducting polymers, there are many parameters to be optimized. There is a molecular weight range suitable for efficient charge carrier mobilities. It was shown that the high planarity of the main chain backbone is key to achieving crystalline thin films. In addition, polymer packing orientations were tuned by side chain engineering. Recently, the effects of doping and additives have also been investigated, and it was found that the addition of quaternary ammonium salts lowered the contact resistance between the organic semiconductor layer and the source and drain electrodes, leading to an increase in the carrier injection efficiency [29–32]. Combinations of molecular design and device engineering will further enhance the

**Fig. 7** **a** Synthesis of the all-acceptor polymer **P2** by direct arylation polymerization. **b** Time-dependent mobility change for the transistor based on **P2** during storage under ambient conditions. **c** Operational stability of the transistor based on **P2** [18]. Copyright 2019 Wiley

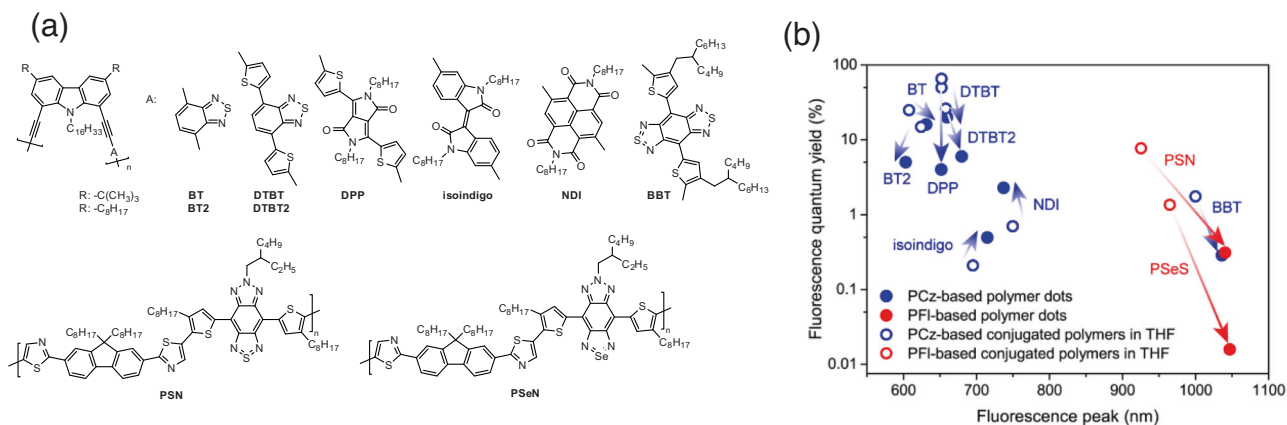
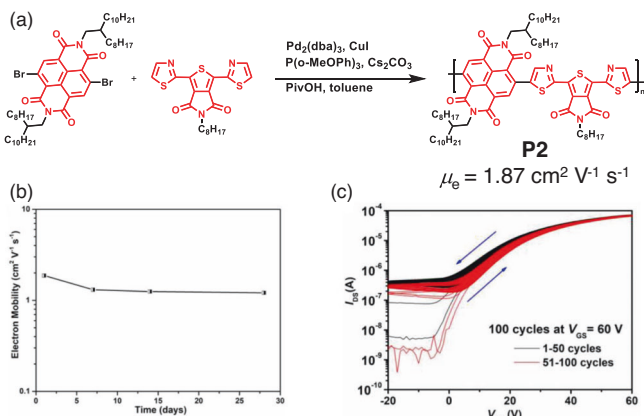


**Fig. 8** **a** Chemical structures of 1,8-carbazole-based donor-acceptor copolymers and the control polymers **PSN** and **PSeS** and **b** the correlations between fluorescence wavelengths and quantum yields in THF solutions and nanoparticles [28]. Copyright 2020 American Chemical Society

capabilities of organic transistors. Moreover, it was demonstrated that these high-mobility polymers are also useful for all-polymer solar cells [33–35] and perovskite solar cells [36, 37].

BBT-based conjugated polymers were initially investigated in thin film transistors. However, recent interest has been directed toward luminescence in the near-infrared region. The original design of nonplanar backbone structures based on the 1,8-carbazole unit was shown to have a significant advantage in suppressing aggregation-induced quenching of conjugated polymers even in the near-infrared range. 1,8-Carbazole-based donor-acceptor copolymers are thus promising for further bioimaging applications.

**Acknowledgements** The author thanks the many collaborators listed in the references.

## Compliance with ethical standards

**Conflict of interest** The author declares no competing interests.

**Publisher's note** Springer Nature remains neutral with regard to jurisdictional claims in published maps and institutional affiliations.

**Open Access** This article is licensed under a Creative Commons Attribution 4.0 International License, which permits use, sharing, adaptation, distribution and reproduction in any medium or format, as long as you give appropriate credit to the original author(s) and the source, provide a link to the Creative Commons license, and indicate if changes were made. The images or other third party material in this article are included in the article's Creative Commons license, unless indicated otherwise in a credit line to the material. If material is not included in the article's Creative Commons license and your intended use is not permitted by statutory regulation or exceeds the permitted use, you will need to obtain permission directly from the copyright holder. To view a copy of this license, visit <http://creativecommons.org/licenses/by/4.0/>.

## References

1. Wang Y, Michinobu T. Rational design strategies for electron-deficient semiconducting polymers in ambipolar/n-channel organic transistors and all-polymer solar cells. *J Mater Chem C*. 2018;6:10390–410.
2. Kim G, Kang SJ, Dutta GK, Han YK, Shin TJ, Noh YY, et al. A thienoisindigo-naphthalene polymer with ultrahigh mobility of 14.4 cm<sup>2</sup>/V·s that substantially exceeds benchmark values for amorphous silicon semiconductors. *J Am Chem Soc*. 2014;136:9477–83.
3. Osaka I, Saito M, Koganezawa T, Takimiya K. Thiophene-thiazolothiazole copolymers: significant impact of side chain composition on backbone orientation and solar cell performances. *Adv Mater*. 2014;26:331–8.
4. Wang Y, Hasegawa T, Matsumoto H, Mori T, Michinobu T. High-performance n-channel organic transistors using high-molecular-weight electron-deficient copolymers and amine-tailed self-assembled monolayers. *Adv Mater*. 2018;30:1707164.
5. Tran DK, Robitaille A, Hai JJ, Lin CC, Kuzuhara D, Koganezawa T, et al. Unified understanding of molecular weight dependence of electron transport in naphthalene diimide-based n-type semiconducting polymers. *Chem Mater*. 2022;34:9644–55.
6. Ono K, Tanaka S, Yamashita Y. Benzobis(thiadiazole)s containing hypervalent sulfur atoms: novel heterocycles with high electron affinity and short intermolecular contacts between heteroatoms. *Angew Chem Int Ed*. 1994;33:1977–9.
7. Yuen JD, Fan J, Sekfiter J, Lim B, Hufschmid R, Heeger AJ, et al. High performance weak donor-acceptor polymers in thin film transistors: effect of the acceptor on electronic properties, ambipolar conductivity, mobility, and thermal stability. *J Am Chem Soc*. 2011;133:20799–807.
8. Fan J, Yuen JD, Wang M, Seifiter J, Seo JH, Mohebbi AR, et al. High-performance ambipolar transistors and inverters from an ultralow bandgap polymer. *Adv Mater*. 2012;24:2186–90.
9. Fan J, Yuen JD, Cui W, Seifiter J, Mohebbi AR, Wang M, et al. High-hole-mobility field-effect transistors based on co-benzobisthiadiazole-quaterthiophene. *Adv Mater*. 2012;24:6164–8.
10. Wang Y, Kadoya T, Wang L, Hayakawa T, Tokita M, Mori T, et al. Benzobisthiadiazole-based conjugated donor-acceptor polymers for organic thin film transistors: effects of  $\pi$ -conjugated bridges on ambipolar transport. *J Mater Chem C*. 2015;3:1196–207.
11. Wang Y, Masunaga H, Hikima T, Matsumoto H, Mori T, Michinobu T. New semiconducting polymers based on benzobisthiadiazole analogues: tuning of charge polarity in thin film transistors via heteroatom substitution. *Macromolecules*. 2015;48:4012–23.
12. Wang Y, Hasegawa T, Matsumoto H, Mori T, Michinobu T. D-A<sub>1</sub>-D-A<sub>2</sub> backbone strategy for benzobisthiadiazole based n-channel organic transistors: clarifying the selenium substitution effect on the molecular packing and charge transport properties in electron-deficient polymers. *Adv Funct Mater*. 2017;27:1701486.
13. Wang Y, Hasegawa T, Matsumoto H, Michinobu T. Significant improvement of unipolar n-type transistor performances by manipulating the coplanar backbone conformation of electron-deficient polymers via hydrogen-bonding. *J Am Chem Soc*. 2019;141:3566–75.
14. Otep S, Wang Y, Kohara A, Matsumoto H, Mori T, Michinobu T. Tuning backbone planarity in thiadiazolobenzotriazole-bis(thienothiophenyl)ethylene copolymers for organic field-effect transistors. *ACS Appl Polym Mater*. 2019;1:2302–12.
15. Osaka I, Saito M, Mori H, Koganezawa T, Takimiya K. Drastic change of molecular orientation in a thiazolothiazole copolymer by molecular-weight control and blending with PC<sub>61</sub>BM leads to high efficiencies in solar cells. *Adv Mater*. 2012;24:425–30.
16. Wang Y, Hasegawa T, Matsumoto H, Mori T, Michinobu T. Rational design of high-mobility semicrystalline conjugated polymers with tunable charge polarity: beyond benzobisthiadiazole-based polymers. *Adv Funct Mater*. 2017;27:1604608.
17. Zhou K, Dong H, Zhang H, Hu W. High performance n-type and ambipolar small organic semiconductors for organic thin film transistors. *Phys Chem Chem Phys*. 2014;16:22448–57.
18. Yang W, Hasegawa T, Matsumoto H, Michinobu T. Significant difference in semiconducting properties of isomeric all-acceptor polymers synthesized via direct arylation polycondensation. *Angew Chem Int Ed*. 2019;58:11893–902.
19. Kimpel J, He W, Cheng Y, Michinobu T. A route to conjugated monomers and polymers incorporating 2,5-connected oxazole in the backbone. *J Org Chem*. 2022;87:9384–90.
20. Watanabe N, He W, Nozaki N, Matsumoto H, Michinobu T. Benzothiadiazole versus thiazolobenzotriazole: a structural study of electron acceptors in solution-processable organic semiconductors. *Chem Asian J*. 2022;17:e202200768.
21. Burroughes JH, Bradley DDC, Brown AR, Marks RN, Mackay K, Friend RH, et al. Light-emitting diodes based on conjugated polymers. *Nature*. 1990;347:539–41.
22. Tane S, Michinobu T. Cu(I)-catalyzed azide-alkyne cycloaddition synthesis and fluorescent ion sensor behavior of carbazole-triazole-fluorene conjugated polymers. *Polym Int*. 2020;70:432–6.

23. Kimpel J, Yoshitake Y, Michinobu T. Poly(3,9-carbazole): a chemically stable extended form of polyaniline for nitro-aromatic sensor applications. *Bull Chem Soc Jpn.* 2020;93:1361–5.
24. Michinobu T, Osaka H, Shigehara K. Alkyne-linked poly(1,8-carbazole)s: a novel class of conjugated carbazole polymers. *Macromol Rapid Commun.* 2008;29:111–6.
25. Michinobu T, Osako H, Shigehara K. Synthesis and properties of conjugated poly(1,8-carbazole)s. *Macromolecules.* 2009;42:8172–80.
26. Michinobu T, Osako H, Seo C, Murata K, Mori T, Shigehara K. Multicolor emission and thin film transistor properties of 1,8-diethynylcarbazole-based conjugated copolymers. *Polymer.* 2011;52:5756–63.
27. Piwoński H, Michinobu T, Habuchi S. Controlling photophysical properties of ultrasmall conjugated polymer nanoparticles through polymer chain packing. *Nat Commun.* 2017;8:15256.
28. Piwoński H, Li W, Wang Y, Michinobu T, Habuchi S. Improved fluorescence and brightness of near-infrared and shortwave infrared emitting polymer dots for bioimaging applications. *ACS Appl Polym Mater.* 2020;2:569–77.
29. Liu Q, Wang Y, Kohara A, Matsumoto H, Manzhos S, Feron K, et al. Tuning the charge carrier polarity of organic transistors by varying the electron affinity of the flanked units in diketopyrrolopyrrole-based copolymers. *Adv Funct Mater.* 2020;30:1907452.
30. Otep S, Lin YC, Matsumoto H, Mori T, Wei KH, Michinobu T. Diketopyrrolopyrrole-thiophene-methoxythiophene based random copolymers for organic field effect transistor applications. *Org Electron.* 2020;87:105986.
31. Liu Q, He W, Shi Y, Otep S, Tan WL, Manzhos S, et al. Directional carrier polarity tunability in ambipolar organic transistors based on diketopyrrolopyrrole and bithiophene imide dual-acceptor semi-conducting polymers. *Chem Mater.* 2022;34:3140–51.
32. He W, Liu Q, Otep S, Matsumoto H, Manzhos S, Sonar P, et al. Tetramethylammonium iodide additive for enhancing the charge carrier mobilities of diketopyrrolopyrrole-based conjugated polymer in ambipolar organic field-effect transistors. *Chin J Chem.* 2023;41:1028–36.
33. Otep S, Tseng YC, Yomogita N, Chang JF, Chueh CC, Michinobu T. Coil-rod-coil triblock copolymers synthesized by macromolecular clicking and their applications for all-polymer solar cells. *J Mater Chem C* 2022;10:346–59.
34. Wang Y, Kim SW, Lee J, Matsumoto H, Kim BJ, Michinobu T. Dual imide-functionalized unit-based regioregular D-A<sub>1</sub>-D-A<sub>2</sub> polymers for efficient unipolar n-channel organic transistors and all-polymer solar cells. *ACS Appl Mater Interfaces.* 2019;11:22583–94.
35. Kim SW, Wang Y, You H, Lee W, Michinobu T, Kim BJ. Impact of incorporating nitrogen atoms in naphthalenediimide-based polymer acceptors on the charge generation, device performance, and stability of all-polymer solar cells. *ACS Appl Mater Interfaces.* 2019;11:35896–903.
36. Said AA, Xie J, Wang Y, Wang Z, Zhou Y, Zhao K, et al. Efficient inverted perovskite solar cells by employing n-type (D-A<sub>1</sub>-D-A<sub>2</sub>) polymers as electron transporting layer. *Small.* 2019;15:1803339.
37. Liu W, Yu F, Wang Y, Michinobu T, Fan W, Zhang Q. Selenium-based solar cell with conjugated polymers as both electron and hole transport layers to realize high water tolerance as well as good long-term and thermal stability. *Sol RRL.* 2020;4:2000425.



Tsuyoshi Michinobu was born 1976 in Hiroshima, studied chemistry at Waseda University and received his PhD under the guidance of Prof. H. Nishide in 2003. After postdoctoral studies at ETH Zurich with Prof. F. Diederich and at the National Institute for Materials Science (NIMS) with Prof. K. Ariga, he joined Tokyo University of Agriculture and Technology as a Research Associate in 2006. He moved to Tokyo Institute of Technology as Assistant Professor in 2008 and was promoted to Associate Professor in 2012 and to Professor in 2023. He received the Showa Denko Materials Award (the Society of Polymer Science, Japan) in 2021.